Proceedings of the 13th
KACC, October 1998

Ball-Handling Control of 14-DOF Pneumatic Dual Manipulator by Position Based Impedance Control

Masanobu NAGATA*, Atsushi OHTOMO*, Zenta IWAI and Hiroya UCHIDA*****

*** Applied Electronics Research Center, Kumamoto Technopolis Foundation**

2081-10 Tabaru, Mashiki-machi, Kamimashiki-gun, Kumamoto 861-2202, JAPAN

Tel : +81-96-286-3300

Fax : +81-96-286-9633

E-mail : nobu@kmt-technopolis.or.jp

**** Department of Mechanical Engineering and Materials Science, Kumamoto University**

***** ISEKI &CO., Ltd.**

Abstract

Robots utilized in the field of welfare or agriculture should be light in weight and flexible in structure. A pneumatic actuator has properties such that it is more powerful compared with a motor of same weight, and that it is flexible, clean and unexplosive.

In this paper we propose a new structure of the pneumatic actuator with two-degree-of-freedom. By using proposed pneumatic actuators, we can easily construct multi-degree-of-freedom pneumatic manipulators. Here we constructed a fourteen-degree-of-freedom pneumatic dual manipulator. The performance of the dual manipulators is confirmed through experiments for ball-handling with impedance control. In the experiments several control schemes, including the decentralized control and the simple adaptive control (SAC), were used. The results show that a flexibility of the pneumatic actuator is appropriate to accomplish the coordinative motion of the right and left arms of the robot.

1. Introduction

The pneumatic actuator has properties that are more powerful compared to a servo-motor of the same weight. It is also flexible, clean and unexplosive. However, it has nonlinear properties because of its compressibility of air and long delay of response. Therefore, it is difficult to design a controller for the pneumatic actuator. In spite of such difficulties, studies with respect to the pneumatic actuator have been considered from various research points of view in order to improve controllability of precision [1],[2]. As second concern is that a structural idea is required to construct manipulators which have more than 6-DOF without losing required moving range since the air cylinder which is most generally used in pneumatic actuators basically has one degree of freedom.

In this paper, we consider both the structure and the control system of the manipulator using pneumatic actuators for applying it to new fields of agriculture or welfare. We propose a 14-DOF pneumatic dual manipulator with two 7-DOF arms, which is constructed by connecting 2-DOF pneumatic actuators in series. This 2-DOF pneumatic actuator that is free for rotation and bending consist of two basic components which will be called "twin pneumatic cylinder". We apply impedance control to the proposed 14-DOF dual manipulator and confirm their control performance by an experiment of ball-handling. Generally speaking, coordinate motion of dual manipulators require exact force control of each end effector. In the experiment, we show that a flexibility of the pneumatic actuator is appropriate to accomplish the sufficient coordinate motion by impedance control of each arm without coordinate control.

This paper is organized as follows. In Section 2, the structure and impedance control model of the proposed 14-DOF pneumatic dual manipulator which has two 7-DOF arms are presented. In Section 3, we propose a 2-DOF pneumatic actuator and show the relation concerning force-balance of air cylinders. The control law for the subsystems of 14-DOF pneumatic dual manipulator is derived in Section 4. The position-based impedance control law is used for each arm. The position control for the arm is accomplished by the simple adaptive control (SAC) method stated as follows. That is, each arm can be divided into a two-input/single-output subsystem including a twin pneumatic cylinder and four-input/two-output subsystems including the 2-DOF pneumatic actuator. To realize those two types of subsystems in the form of single-input/output system and two-input/output system, respectively, we impose a simple assumption on the pneumatic control part. Finally, in Section 5, we show experimental results of ball-handling by the 14-DOF pneumatic dual manipulator with proposed control system.

2. 14-DOF Pneumatic Dual Manipulator

A Structure of 14-DOF Pneumatic Dual Manipulator

The 14-DOF pneumatic dual manipulators proposed here is constructed by connecting one twin pneumatic cylinder and three 2-DOF pneumatic actuators in series. Fig.1 shows the external feature of the 14-DOF pneumatic dual manipulator and a structure of the left arm is illustrated in Fig.2. The right arm is symmetric to the left one with respect to XZ plane of

Cartesian coordinate. As shown in Fig.2, a rotation(θ_{l1}) in the shoulder corresponds to the twin pneumatic cylinder and other 6-DOF corresponds to three 2-DOF pneumatic actuators. Table 1 shows the length for each part in Fig.2.

Table 1 Length of Left Arm

	Ll1	*Ll2*	*Ll3*	*Ll4*	*Ll5*	*Ll6*	*Ll7*	*Ll8*
Length <mm>	225	176	810	140	517	430	140	82

Impedance Control of the Arm

Here we consider impedance control of ball-handling using the proposed 14-DOF pneumatic dual manipulator. In the handling control using dual manipulators, generally, it is a problem how each arm should be coordinated during the manipulating tasks. If high stiffness manipulators are used, output forces of each arm must be controlled exactly. On the other hand, in the case of using the pneumatic actuator, high precision position control may be difficult because the pneumatic actuator has flexibility. However, this flexibility of the actuator gives some advantages with respect to coordinate control or force control. For example, for ball-handling, we can adopt position-based impedance control for each arm without exact coordinate control [3].

Now, we consider position-based impedance control for each left and right arm, independently. Generally speaking, the equation of motion for 7-DOF manipulator except for the part of the joints is expressed by

$$\tau = M(\theta)\ddot{\theta} + h(\theta,\dot{\theta}) + g(\theta) \quad \cdots(1)$$

$\theta = [\theta_1 \cdots \theta_7]^T$ θ_i : i-th joint angle

$M(\theta) \in \Re^{7\times7}$: inertia matrix

$h(\theta,\dot{\theta}) \in \Re^7$: centrifugal and Coriolis vector

$g(\theta) \in \Re^7$: gravitational vector

$\tau = [\tau_1 \cdots \tau_7]^T$, τ_i : i-th joint torque

Further, consider the vector $\theta_m(t)$ of the following impedance model which the joint angle vector θ in (1) is required to follow:

$$M_m \ddot{y}_m(t) + D_m \dot{y}_e(t) + K_m y_e(t) = F^* - F$$

$$\dot{\theta}_m(t) = J^+(\theta_m)\dot{y}_m(t) \quad \cdots(2)$$

$y_m(t)$: trajectory of the impedance model on Cartesian coordinate$\in \Re^6$

$y_e(t) = y_m(t) - y_d(t)$, $y_d(t)$: trajectory of the reference model on Cartesian coordinate$\in \Re^6$

M_m, D_m, K_m : parameters of the impedance model$\in \Re^{6\times6}$

F^* : reference forces for end effector$\in \Re^6$

F : real forces at end effector$\in \Re^6$

$J^+(\theta_m)$: pseudo-inverse Jacobian matrix $\in \Re^{7\times6}$

Position control is used so that the joint angle vector θ will follow $\theta_m(t)$. However, eq.(1) is a complex nonlinear equation. Thus we divide each arm into several subsystems as shown in Fig.2 and apply a decentralized control technique to the position control of each subsystem [4].

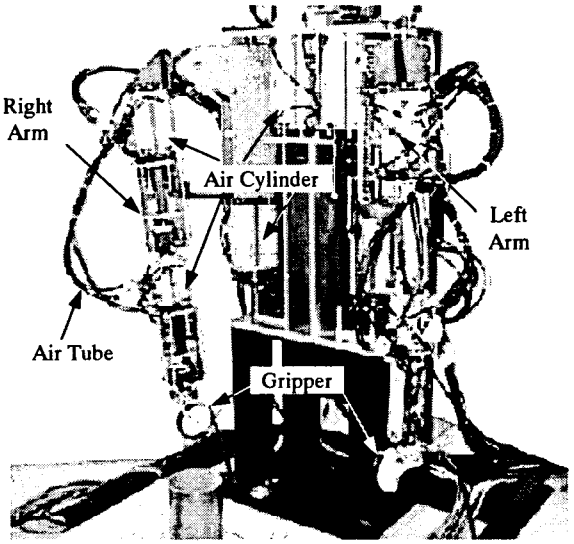

Fig.1 Proposed 14-DOF Pneumatic Dual Manipulators

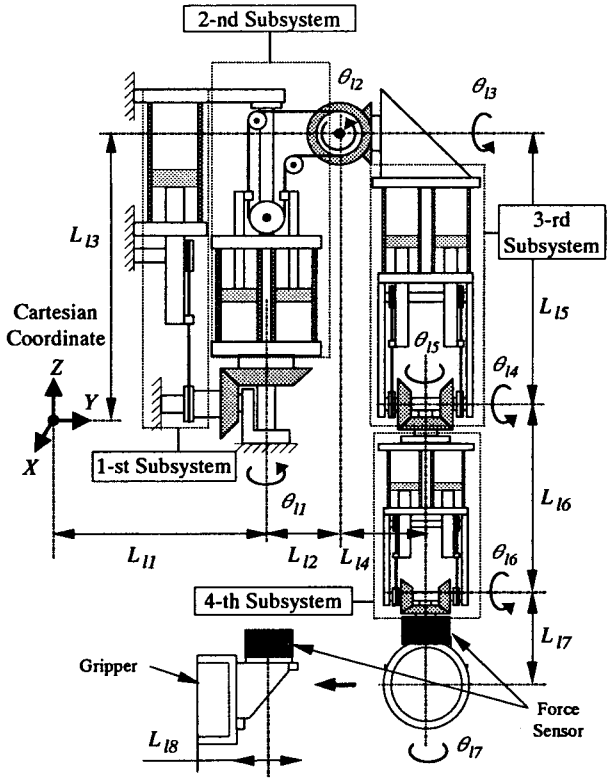

Fig.2 Schematic Diagram of Left Arm

Eq.(1) can be divided into the following subsystems.

$$\tau^j = M^{jj}(\theta)\ddot{\theta}^j + g^j(\theta) + q^j(\theta,\dot{\theta},\ddot{\theta}),\ j = 1\cdots4 \quad \cdots(3)$$

τ^j : joint torque of j-th subsystem , $\tau^1 \in \Re^1, \tau^j|_{j\geq2} \in \Re^2$

θ^j : joint angle of j-th subsystem , $\theta^1 \in \Re^1, \theta^j|_{j\geq 2} \in \Re^2$

$M^{jj}(\theta)$: jj-th minor matrix of $M(\theta)$

$M^{11}(\theta) \in \Re^1, M^{jj}(\theta)|_{j\geq 2} \in \Re^{2\times 2}$

$g^j(\theta)$: j-th element vector of $g(\theta)$

$g^1(\theta) \in \Re^1, g^j(\theta)|_{j\geq 2} \in \Re^2$

where,

$$q^j(\theta,\dot{\theta},\ddot{\theta}) = \sum_{k=1,k\neq j}^{4} \{M^{jk}(\theta)\ddot{\tilde{\theta}}^k\} + h^j(\theta,\dot{\theta}) \quad \cdots(4)$$

$h(\theta,\dot{\theta})$: j-th element vector of $h^j(\theta,\dot{\theta})$

$h^1(*) \in \Re^1, h^j(*)|_{j\geq 2} \in \Re^2$

$M^{jk}(\theta)$: jk-th minor matrix of $M(\theta)$

$M^{1k}(\theta) \in \Re^{1\times 2}, M^{k1}(\theta) \in \Re^{2\times 1}$

$M^{jk}(\theta)\big|_{j\geq 2,k>1} \in \Re^{2\times 2}, \tilde{\theta}^{kT} = \left[\theta^1 \cdots \theta^{k-1}\theta^{k+1} \cdots \theta^4\right]$

$q^j(\theta,\dot{\theta},\ddot{\theta})$ gives interconnection between subsystems. The subsystem for j=1 includes one twin pneumatic cylinder. In the next section, we will describe a 2D-O-F pneumatic actuator that constructs subsystems.

3. 2-DOF Pneumatic Actuator

A Structure and Control System of 2-DOF Pneumatic Actuator

A 2-DOF pneumatic actuator is illustrated in Fig.3 and a pneumatic control system for twin pneumatic cylinder is illustrated in Fig.4. As shown in Figs.3 and 4, a pair of cylinders are connected by two sprockets and a chain antagonistically. An air tube connects cambers which have a push-pull relation in each cylinder. The valve angle regulation using the signal of corresponding pressure sensor controls camber pressure by a PID control algorithm on a specialized micro-computer (Z80) board.

Dynamics of Twin Pneumatic Cylinder

In this subsection, we derive the dynamics of the twin pneumatic cylinder. As stated above, Fig.4 shows the structure of the twin pneumatic cylinder. Here, output forces F_a , F_b of each cylinder are represented by

$$F_a = A_{a2}P_2 - A_{a1}P_1 + (A_{a1} - A_{a2})P_a + A_l P_a$$
$$F_b = A_{b1}P_1 - A_{b2}P_2 + (A_{b2} - A_{b1})P_a + A_l P_a \quad \cdots(5)$$

P_a : Atmosphere pressure

Here, $P_1 = \Delta P_1 + P_{10}$, $P_2 = \Delta P_2 + P_{10} + \Delta P_{20}$, $A_1 = A_{a1} + A_{b1}$, $A_2 = A_{a2} + A_{b2}$, $A = A_1 + A_2$, ΔP_i is variable to pressure, P_{j0} is initial pressure of P_j and ΔP_{20} is the difference between P_{20} and P_{10} . Further suppose that we use cylinders on the same specification, so that $A_1 = A_2$, $A = 2A_1$. Finally, we can obtain the following expression with respect to the output torque of the twin pneumatic cylinder.

$$\tau = Ar\Delta P_2 - A_1 r(\Delta P_2 + \Delta P_1) + A_1 r\Delta P_{20} \quad \cdots(6)$$

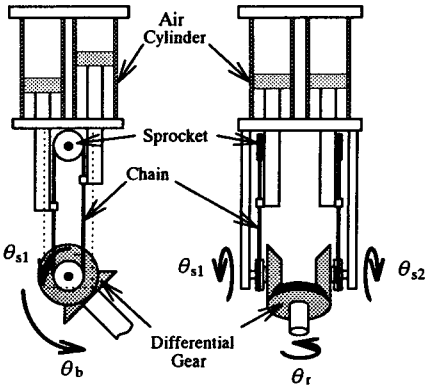

Fig.3 Schematic Diagram of 2-DOF Pneumatic Actuator

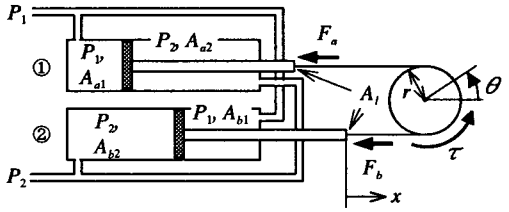

P_*: Pressure of Camber, A_*: Cross-sectional Aria,
θ: rotary angle of sprocket,
r: radius of sprocket

Fig.4 Twin Pneumatic Cylinder

Dynamic Model of Subsystems

For the subsystems($j \geqq 2$) in (3), we will derive the equation of motion including pneumatic actuator. Let τ_r be rotational torque and τ_b be bending torque corresponding to θ_r and θ_b , respectively, as in Fig.3, then, we obtain the following relation for the subsystem.

$$\tau^j = [\tau_b{}^j \quad \tau_r{}^j]^T, \theta^j = [\theta_b{}^j \quad \theta_r{}^j]^T, j \geq 2 \quad \cdots(7)$$

As shown in Figs.3 and 4, the 2-DOF pneumatic actuator is a four-input/two-output interconnected system of which inputs are command values ΔP_i (i=1, $\cdots$,4) and outputs are rotational and bending angles θ_r , θ_b of the differential gear. Then we first consider the transform of forces at the differential gear and derive the equation of motion for each subsystem. Figs.5 and 6 illustrate the transform mechanism of forces at the differential gear. Here, torque τ_{s1} and τ_{s2} are inputs for ① and ② respectively, and rotational and bending angle θ_r and θ_b of ③ are outputs. Further, f_1 , f_2 are forces which effect between these wheels. Here, the same standard wheels are used and four cylinders have the same specification. Equations of motion for each twin pneumatic cylinder with a wheel in the differential gear are described from Fig.6 as:

$$I_s\ddot{\theta}_{s1} = \tau_{s1} - f_1 r - c_1\dot{\theta}_{s1} - F_{s1}$$
$$I_s\ddot{\theta}_{s2} = \tau_{s2} - f_2 r - c_2\dot{\theta}_{s2} - F_{s2} \quad \cdots(8)$$
$$I_s = I_t + m_r r, F_{s*} = F_{t*} + f_{s*} r,$$

I_t : moment of inertia for wheel and sprockets

m_r : mass of cylinder rod, chain and others

F_{f*} : frictional torque of wheel

f_{s*} : friction forces of cylinder, c_* : all of viscosity coefficient

On the other hand, from Fig.5, rotational and bending torque τ_r and τ_b are represented as

$$\tau_r = (f_2 - f_1)r - c_r \dot{\theta}_r - F_{rr}$$

$$\tau_b = (f_1 + f_2)r - c_b \dot{\theta}_b - F_{rb} \quad \cdots(9)$$

c_*: viscosity coefficient, F_{r*}: frictional torque

Since, θ_{s1} , θ_{s2} satisfy the following relation:

$$\theta_{s1} = \theta_b - \theta_r \,, \theta_{s2} = \theta_r + \theta_b \quad \cdots(10)$$

and we can assume $c_1 \cong c_2$ because cylinders and wheels have same standards. Therefore, from (6),(8),(9) and (10),

$$\begin{aligned}\tau_b &= Ar(\Delta P_2 + \Delta P_4) - A_1 r(\Delta P_1 + \Delta P_2 + \Delta P_3 + \Delta P_4) \\ &\quad - 2I_s \ddot{\theta}_b - (c_1 + c_2 + c_b)\dot{\theta}_b \\ &\quad - F_{s1} - F_{s2} - F_{rb} + A_1 r(\Delta P_{20} + \Delta P_{40}) \\ \tau_r &= -Ar(\Delta P_2 - \Delta P_4) + A_1 r(\Delta P_1 + \Delta P_2 - \Delta P_3 - \Delta P_4)_r \\ &\quad - 2I_s \ddot{\theta}_r - (c_1 + c_2 + c_r)\dot{\theta} \\ &\quad + F_{s1} - F_{s2} - F_{rr} - A_1 r(\Delta P_{20} - \Delta P_{40}) \quad \cdots(11)\end{aligned}$$

are obtained. Finally, from (3), (7) and (11), the equation of motion for j-th($j \geqq 2$) subsystem is given by

$$\ddot{\theta}^j = -\tilde{M}^{jj}(\theta)^{-1} V^j \dot{\theta}^j + \tilde{M}^{jj}(\theta)^{-1} R^j u^j(t) + w^j(t) \quad \cdots(12)$$

$$u^j(t) = \left[\Delta P_1^{\,j} \quad \Delta P_2^{\,j} \quad \Delta P_3^{\,j} \quad \Delta P_4^{\,j}\right]^T$$

$$R^j = \begin{bmatrix} -A_1^{\,j} r^j & (A^j - A_1^{\,j}) r^j & -A_1^{\,j} r^j & (A^j - A_1^{\,j}) r^j \\ A_1^{\,j} r^j & -(A^j - A_1^{\,j}) r^j & -A_1^{\,j} r^j & (A^j - A_1^{\,j}) r^j \end{bmatrix}$$

$$\tilde{M}^{jj}(\theta) = \begin{bmatrix} m_{11}^{\,jj}(\theta) + 2I_s^j & 0 \\ 0 & m_{22}^{\,jj}(\theta) + 2I_s^j \end{bmatrix} > 0$$

$$w^j(t) = \tilde{M}^{jj}(\theta)^{-1}\{f^j - g^j(\theta) - \tilde{q}^j(\theta, \dot{\theta}, \ddot{\theta})\}$$

$$\tilde{q}^j(\theta, \dot{\theta}, \ddot{\theta}) = q^j(\theta, \dot{\theta}, \ddot{\theta}) + [m_{12}^{\,jj}(\theta)\ddot{\theta}_r^j \quad m_{21}^{\,jj}(\theta)\ddot{\theta}_b^j]^T$$

$m_{lm}^{\,jj}(\theta)$:lm–th elements of $M^{jj}(\theta)$

$$V^j = \begin{bmatrix} c_1^{\,j} + c_2^{\,j} + c_b^{\,j} & 0 \\ 0 & c_1^{\,j} + c_2^{\,j} + c_r^{\,j} \end{bmatrix}$$

$$f^j = \begin{bmatrix} -F_{s1}^{\,j} - F_{s2}^{\,j} - F_{rb}^{\,j} + A_1^{\,j} r^j (\Delta P_{20}^{\,j} + \Delta P_{40}^{\,j}) \\ F_{s1}^{\,j} - F_{s2}^{\,j} - F_{rr}^{\,j} - A_1^{\,j} r^j (\Delta P_{20}^{\,j} - \Delta P_{40}^{\,j}) \end{bmatrix}$$

As the result, we can see from (12) that the subsystems of $j \geqq 2$ are the four-input/two-output nonlinear systems which have interactions and disturbances. Similarly, for the subsystem of j=1, we can obtain the two-input/single-output nonlinear system.

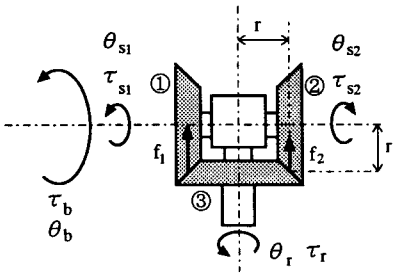

Fig.5 Transform of Torque and Forces at Differential Gear

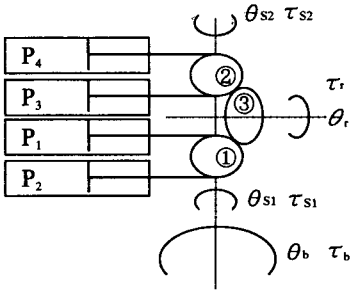

Fig.6 2-DOF Pneumatic Actuator

4. Design of control System

In this section, we consider a control system for subsystems of $j \geqq 2$ represented by (12). Here, we impose a following assumption in order to make the number of inputs equal to the number of outputs.

[Assumption 1]
Response of pressure control system to adjust air pressure in camber of cylinder is sufficiently fast compared with the command value of corresponding pressure.

From Assumption 1, we can ignore the dynamics of air pressure. Thus, with respect to pressure variable $\Delta P_i^{\,j}$ and the command value of pressure $\Delta P_i^{\,j*}$ (i=1~4), $\Delta P_i^{\,j} \cong \Delta P_i^{\,j*}$ holds. Further, let us define new variable $\Delta P_{ci}^{\,j*}$ (i=1,2) as follows:

$$\Delta P_{c1}^{\,j*} = -\Delta P_1^{\,j*} = \Delta P_2^{\,j*}, \Delta P_{c2}^{\,j*} = -\Delta P_3^{\,j*} = \Delta P_4^{\,j*} \quad \cdots(13)$$

Eq.(13) implies that if the command value of pressure for camber at the side of P_2 in Fig.3 is defined as ΔP, then, the command value of pressure for camber at the side of P_1 becomes $-\Delta P$. Namely, the number of inputs for a twin pneumatic cylinder becomes one by defining $\Delta P_{ci}^{\,j*}$. It follows that subsystems of $j \geqq 2$ can be represented by the following two-input/output system:

$$\ddot{\theta}^j = -\tilde{M}^{jj}(\theta)^{-1} V^j \dot{\theta}^j + \tilde{M}^{jj}(\theta)^{-1} \tilde{R}^j \tilde{u}^j(t) + w^j(t) \quad \cdots(14)$$

$$\tilde{R}^j = \begin{bmatrix} A^j r^j & A^j r^j \\ -A^j r^j & A^j r^j \end{bmatrix}, \quad \tilde{u}^j(t) = \left[\Delta P_{c1}^{\,j*} \quad \Delta P_{c2}^{\,j*}\right]^T$$

As eq(14) has still interactions and nonlinearlites, one

needs to consider the multi-variable and/or robust control system for controlling the above subsystems. Now, we consider to apply the simple adaptive control (SAC) method to (14).

Here, eq.(14) without disturbances $w^j(t)$ can be described by two-input/output four order state equation as follows:

$$\dot{x}^j(t) = A^j x^j(t) + B^j u^j(t)$$
$$y^j(t) = C x^j(t) \qquad \cdots(15)$$
$$x^j(t) = \left[\theta_r^{\ j} \quad \theta_b^{\ j} \quad \dot{\theta}_r^{\ j} \quad \dot{\theta}_b^{\ j}\right]^T, \ u^j(t) = \left[\Delta P_{c2}^{\ j*} \quad \Delta P_{c1}^{\ j*}\right]^T$$
$$A^j = \begin{bmatrix} \mathbf{0} & \mathbf{I} \\ -a_1^{\ j} & 0 \quad -a_1^{\ j} \quad 0 \\ 0 & -a_2^{\ j} \quad 0 \quad -a_2^{\ j} \end{bmatrix}, \ B^j = \begin{bmatrix} \mathbf{0} \\ -b_1^{\ j} & b_1^{\ j} \\ b_2^{\ j} & b_2^{\ j} \end{bmatrix}$$
$$C = [I \quad 0], \ a_1^{\ j}, a_2^{\ j}, b_1^{\ j}, b_2^{\ j} > 0$$

Generally, in order to apply the SAC to m input/output n order systems, the following four conditions are need [5].

[Condition 1]
The transfer matrix of the plant is minimum-phase.

[Condition 2]
The relative order of the plant is m.

[Condition 3]
$CB > 0$

[Condition 4]
(i) $\det\begin{bmatrix} A & B \\ C & 0 \end{bmatrix} \neq 0$

(ii) reference input $u_r(t)$ is bounded and $\dot{u}_r(t)$ is bounded and piecewise continuous.

(iii) Ω_{11} is the solution of the matrix equation

$$\begin{bmatrix} A & B \\ C & 0 \end{bmatrix}\begin{bmatrix} \Omega_{11} & \Omega_{12} \\ \Omega_{21} & \Omega_{22} \end{bmatrix} = I$$

where no eigenvalue of Ω_{11} is equal to the inverse of an eigenvalue of A_r(:coefficient matrix of reference model)

Eq.(15) does not satisfy above conditions of **2** and **3**. Now, we introduce the following PD compensator $H(s)$ to $u^j(t)$:

$$H(s) = \begin{bmatrix} d_1^{\ j}s + k_1^{\ j} & d_2^{\ j}s + k_2^{\ j} \\ d_3^{\ j}s + k_3^{\ j} & d_4^{\ j}s + k_4^{\ j} \end{bmatrix} \qquad \cdots(16)$$

Here, if $k_1 \sim k_4$ and $d_1 \sim d_4$ satisfy next relations,

$$k_1^{\ j}k_4^{\ j} - k_3^{\ j}k_2^{\ j} < 0, \ k_1^{\ j}d_4^{\ j} + d_1^{\ j}k_4^{\ j} - (k_2^{\ j}d_3^{\ j} + d_2^{\ j}k_3^{\ j}) < 0$$
$$d_1^{\ j}d_4^{\ j} - d_3^{\ j}d_2^{\ j} < 0, \ k_1^{\ j}k_4^{\ j} - k_3^{\ j}k_2^{\ j} < 0$$
$$d_3^{\ j} - d_1^{\ j} > 0, \ d_3^{\ j}d_2^{\ j} - d_1^{\ j}d_4^{\ j} > 0 \qquad \cdots(17)$$

[Condition 2] and **[Condition 3]** are satisfied. With respect to **[Condition 4]**, we suppose that (15) satisfies the condition. Consequently, we adopt SACs with PD compensator $H(s)$ for each subsystem of $j \geqq 2$. Similarly, for the subsystem of

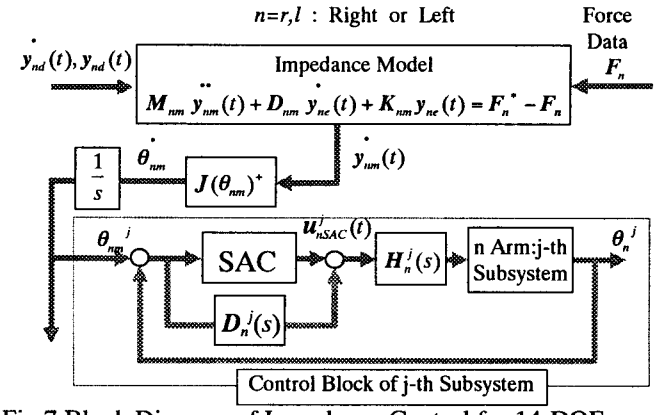

Fig.7 Block Diagram of Impedance Control for 14-DOF Pneumatic Dual Manipulators

j=1, we can obtain a single-input/single-output system. On the other hand, as SAC does not include the integration, the influence of $w^j(t)$, especially the frictional term, might be appeared. Therefore, we will consider to add the integrator to the SAC. Fig.7 illustrates the control block diagram of the position-based impedance control system with SAC loop for each arm. Here, subscript n implies right arm(r) or left arm(l), and $D_n^j(s) = diag[\, i_{n1}^j / s, \ i_{n2}^j / s \,]$. Here, the reference model of SAC is

$$\dot{x}_{nr}^{\ j}(t) = A_{nr}^{\ j} x_{nr}^{\ j}(t) + B_{nr}^{\ j} u_{nr}^{\ j}(t)$$
$$y_{nr}^{\ j}(t) = C_r x_{nr}^{\ j}(t) \qquad \cdots(18)$$

and SAC control inputs $u_{nSAC}^j(t)$ are given as follows.

$$u_{nSAC}^j(t) = K_n^j(t) z_n^j(t) \qquad \cdots(19)$$
$$z_n^j(t) = \left[e_n^j(t)^T \quad x_{nr}^{\ j}(t)^T \quad u_{nr}^{\ j}(t)^T\right]^T$$
$$e_n^j(t) = y_n^j(t) - y_{nr}^{\ j}(t), \ K_n^j(t) = K_{nP}^{\ j}(t) + K_{nI}^{\ j}(t)$$
$$K_{nP}^{\ j}(t) = -e_n^j(t) z_n^j(t)^T \Gamma_{nP}^{\ j},$$
$$\dot{K}_{nI}^{\ j}(t) = -e_n^j(t) z_n^j(t)^T \Gamma_{nI}^{\ j} - \sigma_n^j K_{nI}^{\ j}(t)$$
$$\Gamma_{nP}^{\ j} = \Gamma_{nP}^{\ jT} > 0, \Gamma_{nI}^{\ j} = \Gamma_{nI}^{\ jT} > 0$$

5. Experimental Results

Ball-handling control by the 14-DOF pneumatic dual manipulator has been carried out to confirm an effective way of applying impedance control discussed in this paper. Fig.8 gives trajectory of end effectors for ball-handling. That is, lines ◆◆ in Fig.8 are reference trajectory $y_{rd}(t)$ and $y_{ld}(t)$ in which the dual manipulator grasp a ball in front and move it up/down and release it at the initial position. Where, configuration of both end effectors will be constant through the trajectory. Parameters of this experiment are given as follows:

a. Impedance parameters
・Right arm
$M_{rm} = diag[0.1 \quad 0.75 \quad 5 \quad 10 \quad 10 \quad 10]$<kg>

$D_{rm} = diag[0.9 \quad 2.13 \quad 14.2 \quad 20 \quad 20 \quad 20]$<N/(mm/s)>

$K_{rm} = diag[0.2 \quad 1.5 \quad 10 \quad 10 \quad 10 \quad 10]$<N/mm>

$F_r^* = [0 \quad 90 \quad 0 \quad * \quad * \quad *]^T$ <N>

·Left arm

$M_{lm} = diag[0.1 \quad 0.75 \quad 5 \quad 10 \quad 10 \quad 10]$<kg>,

$D_{lm} = diag[1.5 \quad 2.13 \quad 14.2 \quad 20 \quad 20 \quad 20]$<N/(mm/s)>,

$K_{lm} = diag[1.0 \quad 1.5 \quad 10 \quad 10 \quad 10 \quad 10]$<N/mm>,

$F_l^* = [* \quad -90 \quad 0 \quad * \quad * \quad *]^T$ <N>

b. Parameters of SAC and $D(s)$

·Right arm

$\sigma_r^1 = 0.01, \ \sigma_r^2 = 0.1, \ \sigma_r^3 = 0.2, \ \sigma_r^4 = 0.2$

$\Gamma_{rP}{}^1 = diag[0.1,0.1,0.1], \Gamma_{rP}{}^{j\geq 2} = diag[0.1,0.1,0.1,0.1,0.1,0.1]$

$\Gamma_{rI}{}^1 = diag[1500,0.1,0.1], \ i_{r1}^1 = 3$

$\Gamma_{rI}{}^2 = diag[1000,1000,0.1,0.1,0.1,0.1], \ i_{r1}^2 = 5, \ i_{r2}^2 = 5$

$\Gamma_{rI}{}^3 = diag[500,300,0.1,0.1,0.1,0.1], \ i_{r1}^3 = 2, \ i_{r2}^3 = 2$

$\Gamma_{rI}{}^4 = diag[300,300,0.1,0.1,0.1,0.1], \ i_{r1}^4 = 2, \ i_{r2}^4 = 2$

$K_{rI}{}^1(0) = [-8,0,0], \ K_{rI}{}^2(0) = \begin{bmatrix} -6,0,0,0,0,0 \\ 0,-8,0,0,0,0 \end{bmatrix}$

$K_{rI}{}^3(0) = \begin{bmatrix} -6,0,0,0,0,0 \\ 0,-5,0,0,0,0 \end{bmatrix}, \ K_{rI}{}^4(0) = \begin{bmatrix} -5,0,0,0,0,0 \\ 0,-5,0,0,0,0 \end{bmatrix}$

· Left arm

$\sigma_l^1 = 0.01, \ \sigma_l^2 = 0.1, \ \sigma_l^3 = 0.2, \ \sigma_l^4 = 0.2$

$\Gamma_{lP}{}^1 = diag[0.1,0.1,0.1], \Gamma_{lP}{}^{j\geq 2} = diag[0.1,0.1,0.1,0.1,0.1,0.1]$

$\Gamma_{lI}{}^1 = diag[1500,0.1,0.1], \ i_{l1}^1 = 3$

$\Gamma_{lI}{}^2 = diag[1500,1500,0.1,0.1,0.1,0.1], \ i_{l1}^2 = 5, \ i_{l2}^2 = 5$

$\Gamma_{lI}{}^3 = diag[1500,800,0.1,0.1,0.1,0.1], \ i_{l1}^3 = 4, \ i_{l2}^3 = 4$

$\Gamma_{lI}{}^4 = diag[1000,800,0.1,0.1,0.1,0.1], \ i_{l1}^4 = 2, \ i_{l2}^4 = 1$

$K_{lI}{}^1(0) = [-8,0,0], \ K_{lI}{}^2(0) = \begin{bmatrix} -8,0,0,0,0,0 \\ 0,-8,0,0,0,0 \end{bmatrix}$

$K_{lI}{}^3(0) = \begin{bmatrix} -5,0,0,0,0,0 \\ 0,-7,0,0,0,0 \end{bmatrix}, \ K_{lI}{}^4(0) = \begin{bmatrix} -3,0,0,0,0,0 \\ 0,-3,0,0,0,0 \end{bmatrix}$

c. Others

· Parameters of $H(s)$:

$j = 1$: $k_1 = 1.0, d_1 = 0.001$

$j \geq 2$: $k_1{}^j = -1, k_2{}^j = k_3{}^j = k_4{}^j = 1$

$d_1{}^j = -0.01, d_2{}^j = d_3{}^j = d_4{}^j = 0.01$

· Reference model :

$A_r{}^j = diag[-2.0 \quad -2.0], B_r{}^j = diag[1.0 \quad 1.0], C_r{}^j = I$

$u_r{}^j(t) = \left[(-2.0 * \theta_r{}^j + \dot{\theta}_r{}^j), (-2.0 * \theta_b{}^j + \dot{\theta}_b{}^j) \right]^T$

· Ball : diameter:≒22<cm>, mass:≒3.7 <kg>

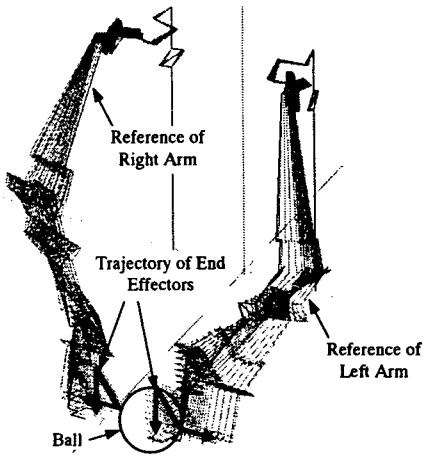

Fig.8 Reference Trajectory for Ball Handling by 14-DOF Pneumatic Dual Manipulators

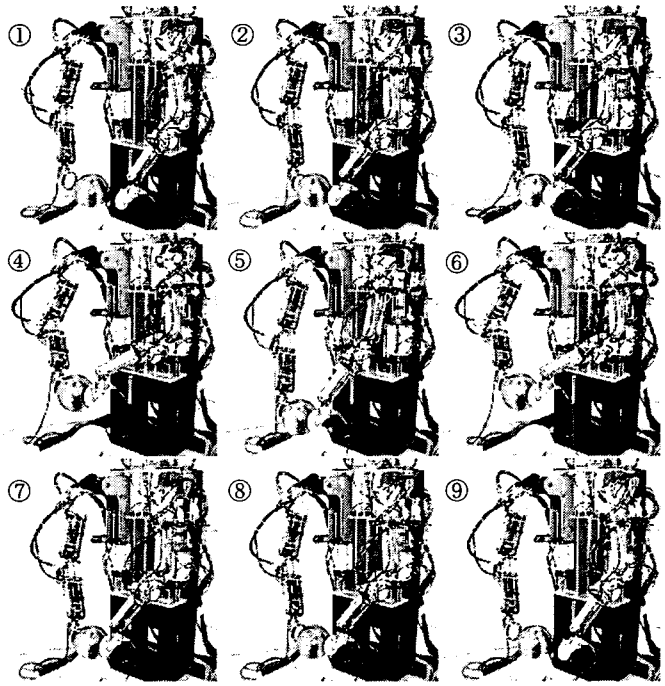

Fig.9 Experiments of Ball Handling Control by 14-DOF Pneumatic Dual Manipulators

· Initial pressure : $P_0 \fallingdotseq 3.92 \times 10^5$ <Pa>

· Calculation of pseudo-inverse Jacobian matrix:[6]

$J^+(\theta_{nm}) = Q^{-1}J(\theta_{nm})^T (J(\theta_{nm})Q^{-1}J(\theta_{nm})^T)^{-1}, n = r, l$

$Q = diag[2.0 \quad 1.0 \quad 1.0 \quad 0.5 \quad 0.5 \quad 0.5 \quad 0.5]$

·Sampling time: 10 <msec>

Concerning F_r^*, F_l^* in **a**, '*' marked elements imply that impedance control is not applied to the corresponding direction. Namely, only position control without impedance control is applied to the orientation of both end effectors and the direction of the X axis in the left arm.

Fig.9 shows a time sequence of photographs in which the proposed 14-DOF dual manipulator was carrying out ball-handling. The dual manipulator was approaching the ball at

② from the initial position ①, and grasp it at ③. And the dual manipulator moved the ball up and down at ④～⑥, put it on the initial position at ⑦, and released it at ⑧, then finally returned to the initial position at ⑨ (= ①) . Correspondingly Fig.9, position errors $e_r(t), e_l(t)$ between trajectories of both end effectors $y_r(t), y_l(t)$ and impedance model $y_{rm}(t), y_{lm}(t)$ are shown in Fig.10. Here, $e_r(t)$, $e_l(t)$ are

$$e_r(t) = y_r(t) - y_{rm}(t) = [erx \quad ery \quad erz \quad *]^T,$$
$$e_l(t) = y_l(t) - y_{lm}(t) = [elx \quad ely \quad elz \quad *]^T \qquad \cdots(20)$$

Moreover Fig.11 illustrates forces working the ball from both end effectors. From Fig.10, it is shown that both end effectors were following impedance models in errors about ±30mm on the average. The reason position errors (*ery,ely*) of the *Y* axis were large, around 85sec, is that the dual manipulator released the ball at that time. Fig.11 shows that forces about 60N～100N from end effectors worked the ball in the direction of the *Y* axis, and that forces about 20N worked the ball in the direction of the *Z* axis in order to lift it.

Although the above mentioned tracking errors are larger compared with conventional manipulators, the dual manipulator achieved a series of motion in ball-handling without dropping the ball. Thus, this experiment gives a possibility that the coordinate motion can be accomplished by making use of a flexibility of pneumatic actuators instead of exact coordinate control.

In the following, we will examine briefly an assumption used in the designing control system for subsystems of the dual manipulator in Section 4. It is possible that pneumatic control by PID using a micro-computer board is approximately regarded to the first order system that has about 200msec～300msec time constant for step input from 1kgf/cm^2 to 5kgf/cm^2. As maximum value of pressure variation in this experiment is about 1 kgf/cm^2/sec, time constant of the first order system is 50msec～70msec. Although we can not affirm immediately from the above mentioned results whether Assumptions 1 is satisfied in this experiment or not, considering the achievement of ball-handling, we can conclude that this assumption is almost satisfied.

6. Conclusions

In this paper, we propose a 14-DOF pneumatic dual manipulator was constructed by connecting the 2-DOF pneumatic actuator and the performance of the dual manipulator was confirmed through experiment concerning ball-handling by impedance control with SAC loop. By this experiment, we could confirm that the coordinate motion can be accomplished without exact coordinate control by utilizing a flexibility of pneumatic actuators.

How to guarantee the stability of all signals in the impedance control system for the dual manipulator from the theoretical viewpoint has remained a problem that should be investigated in the near future.

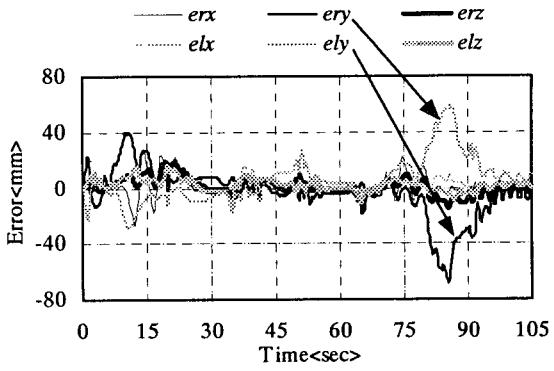

Fig.10 Experimental Results of $e_n(t)$

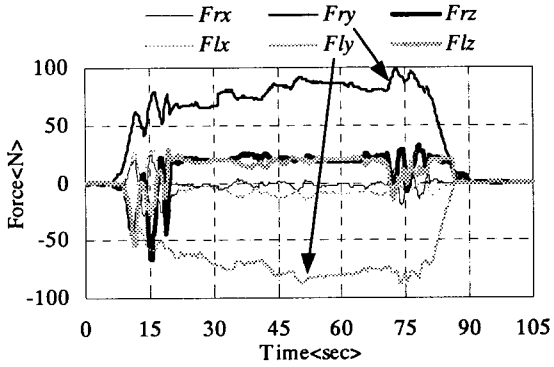

Fig.11 Experimental Results of F_n

References

[1] Noritugu, T. and M.Takaiwa, "Robust Positioning Control of Pneumatic Servo System with Pressure Control Loop," *Proceeding of* 1995 *IEEE International Conference On Robotics and Automation*, Nagoya, Aichi, Japan, pp.2613-2618, 1995.

[2] Badano, F., M.Betemps and D.Thomasset, "Control of a Planar Fine Positioner Actuated by Metal Bellows," *Automatica*, No.30, Vol.11 , pp.1677-1691, 1994.

[3] Lawrence, D.A., "Impedance Control Stability Properties In Common Implementations," *Proceeding of* 1988 *IEEE International Conference On Robotics and Automation*, Philadelphia, Pennsylvania, USA, pp.1185-1190, 1988.

[4] Colbaugh, R., H.Sereji and K.Glass, "Decentralized Adaptive Control of Manipulators," *Journal of Robotics Systems*, No.11, Vol.5, pp.425-440, 1994.

[5] Mizumoto, I., T.Egashira, and Z.Iwai, "Simple Adaptive Control for MIMO Plants with Unmodelled Dynamics and Its Application to Processes with Higher Order Lag Elements," *Proceeding. of IFAC International Symposium on Advanced Control of Chemical Processes*, Banff, Canada, pp.409-414, 1997.

[6] Whitney, D.E., "Resolved Motion Rate Control of Resolved Manipulators and Human Prostheses," *Proceeding of 5th Annual Conference on Manual Control*, Cambridge, MA, USA, pp.685-696, 1996.